

# 910. Numerical modeling of fiber pull-out micromechanics in concrete matrix composites

O. Kononova<sup>1</sup>, V. Lusiš<sup>2</sup>, A. Galushchak<sup>3</sup>, A. Krasnikovs<sup>4</sup>, A. Macanovskis<sup>5</sup>

Riga Technical University, Latvia

E-mail: <sup>1</sup>*olga.kononova@rtu.lv*, <sup>2</sup>*vitalijs.lusis@rtu.lv*, <sup>3</sup>*galushchak.a@gmail.com*,

<sup>4</sup>*akrasn@latnet.lv*, <sup>5</sup>*artursmacanovskis@inbox.lv*

(Received 21 October 2012; accepted 4 December 2012)

**Abstract.** The presented research work compares numerical results of single fiber pull-out of elastic matrix with the experimental data obtained for single steel fiber pulled out of high-strength concrete matrix. The pull-out process was studied by means of accurate 2D elastic and 3D elasto-plastic finite element models taking into account the nonlinearity. Numerical modeling was performed for straight-shaped fiber embedded into the elastic matrix under variable angle with respect to applied pulling force and at variable depth. Friction between fiber and matrix, matrix shrinkage as well as elastic and plastic deformations in the fiber were taken into account. The objective of numerical modeling was to evaluate significance of different phenomena such as friction between steel fiber and concrete matrix, matrix shrinkage and fiber plasticity in a single fiber pull-out process by taking into consideration experimental findings.

**Keywords:** pull-out, finite element method, shrinkage, elasto-plastic fiber.

## Introduction

It is well known that the main disadvantage of concrete is its low tensile strength. Due to this fact, concrete tends to crack even under relatively low forces and for this reason it is used mainly in the form of reinforced concrete. It has been proven by many researchers that the overall behavior of concrete can be improved by the addition of fibers. A wide range of fibers is used for the production of fiber-reinforced concrete (steel, plastic, glass, micro-composite, etc.). Traditional concrete mixing, transportation and molding technologies, used for concretes with dispersed short fibers, allow to fabricate fiber-concrete structural elements with fibers content not exceeding few percent of volume fraction. The positive effect of fibers, in this situation, is not obvious until the first crack occurs in the concrete. After this point, the behavior of fiber reinforced concrete is different from that of unreinforced. Increase of the applied external loads leads to initialization of matrix fracture process: micro-cracks start to open, grow and coalescent finally forming one or few macro-cracks. The fibers are bridging every crack. Here the study will be limited to the use of steel fibers. Focusing on micro-mechanical investigations of single fiber pulling-out process, it is necessary to mention some works. In [1, 2] numerical modeling was performed simulating the pull-out of straight fiber out of a concrete. In [3] FE model approximates the nonlinear behavior of fiber and matrix interface. In [4-6] a detailed 2D and 3D FEM modeling was performed to investigate stress distribution in matrix and fiber during pull out process. Interpretations of interface bond micro-mechanical properties were done by Stang [7], Li [8], Li et al. [9] and Stang et al. [10]. Analytical solution for single fiber pull-out from elastic matrix with friction, in orthogonal direction to elastic volume outer surface, was obtained in [11]. Some additional works have studied behavior of fiber reinforced concrete as well as micro-mechanical parameters that affect steel fiber pull-out process [12-15]. More detailed investigation of elasto-plastic single hooked end fiber pull-out from concrete matrix is presented in [16].

## Experimental investigation

Single fiber-concrete samples were prepared in order to determine fiber pull-out resistance

experimentally [17-20]. The samples were prepared in forms as shown in Fig. 1. A single steel fiber is embedded along vertical symmetry axis of the concrete mold form. A plastic separator was inserted to ensure that the applied force is transferred through the fiber thus causing pull-out,  $l_f$  designates the embedded length of the fiber and  $\alpha$  is the inclination angle of the fiber with respect to the applied pull-out load direction. The shape of test samples was chosen so as to easily fit in the grips of the mechanical tensile testing machine.

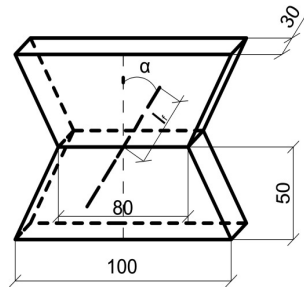


Fig. 1. Configuration of a pull-out test specimen

In [18-20] different geometry fiber types were investigated. Fiber length for all types was 50 mm. For each type of fibers, five different embedded lengths have been observed in the investigation – 25 mm (symmetrical embedding of 50 mm long fiber), 20 mm, 15 mm, 10 mm and 5 mm. In the framework of present investigation, experimental data of pull-out resistance for inclined at different angle to applied pulling out force direction and the effect of embedded fiber length for only straight round cross-section steel fibers with diameter 0.75 mm will be used for comparison with numerical modeling data. For each configuration of fiber matrix alignment a total number of 9 samples were produced thus ensuring adequate statistics of the performed tests.

The pull-out tests were carried out on a tensile testing machine “Zwick/Roell” Z150 at a constant displacement control rate of 10 mm/min. 1 kN load cell was mounted and applied for the performed tests. The pull-out displacement was measured using externally connected video extensometer “Messphysik” measuring the mutual displacement between two reference lines which were drawn onto the surface of the specimen. The reference lines were drawn on a specially prepared surface, which was glued on each specimen. Each test was performed until complete fiber pull-out from the matrix (not in any test fiber rupture was observed). Data of the applied force and corresponding displacement values were automatically synchronized and recorded for each sample.

Analyzing applied force-pulled out displacement curves is easy to conclude that different steel fiber shapes involve different micro-mechanisms in the pull-out process. Initially fibers and the surrounding concrete matrix deform elastically. The linear elastic behavior of the fiber-matrix system is interrupted by interface debonding, which occurs due to overall weak bonding between the concrete matrix and the surface of the steel fiber. This mechanism was numerically investigated using fracture mechanics methods in [21]. Interface shear crack propagates and the interface debonding continues until the whole length of the fiber has parted from the surrounding concrete matrix. At that point the further applied pull-out load is resisted only by friction forces resulting from fiber sliding out of the concrete matrix. If steel fiber has inclined to applied tension direction, much of the pull-out resistance can be achieved from its elasto-plastic straightening. Straightening of steel fibers can only be possible if the surrounding concrete matrix has sufficient strength to resist stress concentration at fiber edges. If surrounding concrete matrix is weak, the stress concentration causes failure of the brittle matrix and no pull-out resistance is obtained. Concrete matrix failure (spalling) is more likely to occur in the case of larger fiber diameters.

## Modeling

### Stresses in single elastic fiber pulling out of elastic volume

We start with the situation when elastic single fiber is oriented orthogonal to elastic volume (concrete) surface and is pulled out. External load is applied to fiber pulling it out of the matrix. Performed analysis of experimental data for glass and carbon fibers was revealed four main stages of such procedure:

- a) fiber and matrix are bonded together (perfect bond), all deformations in the system are elastic;
- b) cylindrical delamination crack is starting from the outer elastic volume surface propagating between fiber and matrix. Crack is growing mainly by fracture mode 2;
- c) when fiber embedment is small (short fiber or pulling out the shorter end of fiber which is bridging the crack) delamination is reaching all length of fiber after that fiber with friction is pulled out. If fiber embedment is large, fiber is breaking at the length  $l_0$  in concrete, after what free fiber end with friction is pulled out of the matrix;
- d) stretched fiber breaks out of concrete. Fibers breaking in material according to scenario (a)-(c) are responsible to fiber-concrete post-cracking quasi-plastic behavior and are the subject of present investigation. 2D simulations have been performed with ANSYS solver.

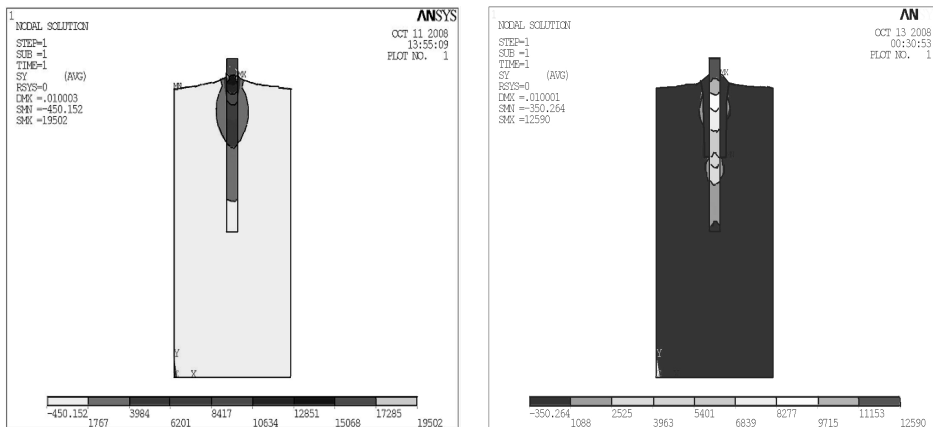


**Fig. 2.** Stress in vertical direction in fiber and concrete matrix (without shrinkage). Single elastic (glass) fiber is embedded into elastic (concrete) matrix with perfect bond between them (left picture). Between pulling out fiber and matrix is growing delamination, which is simulated by thin soft interlayer (right picture)

Mechanical properties of materials correspond to elastic glass fiber pulling out of elastic concrete matrix with: Young modulus of elastic concrete matrix:  $E = 30000$  MPa, Poisson's ratio of concrete matrix  $\nu = 0.2$ ; elastic Young modulus of AR glass fiber:  $E = 70000$  MPa, Poisson's ratio of AR glass fiber  $\nu = 0.2$ ; Young modulus of elastic interlayer between fiber and matrix:  $E = 500-3000$  MPa and its Poisson's ratio  $\nu = 0.25$ . Calculations were carried out for matrix with and without shrinkage.

Three numerical 2D models were under investigation.

First: single elastic (glass) fiber is embedded into concrete matrix with perfect bond between them and subjected to external pulling load. Axial stress contours in vertical direction in concrete and matrix are shown in Fig. 2 (left picture). Maximal tensile stress in stretched fiber is concentrated in cross-section coinciding with concrete outer surface. Similar situation is with shear stress on the interface between matrix and fiber. Shrinkage increases the total level of

acting stresses. The second model describes the situation when delamination is growing between pulling out fiber and matrix. In delaminated area the fiber and matrix are debonded. Each mutual motion in this zone is accompanied by friction. Numerically this situation was simulated incorporating thin soft interlayer between fiber and matrix. Axial stress contours in vertical direction in matrix and fiber are shown in Fig. 2 (right picture). Stresses in fiber along the line parallel to fiber axis in the vicinity of interface with matrix (0.98 of fiber radius) are presented in Fig. 3 (left picture). Peaks on the lines (going from left to right) corresponds to: a) fiber end in concrete (small peaks), b) beginning of delamination zone (middle peaks), c) outer surface of concrete block. Stress peaks at the front of delamination zone (corresponds to singularities in classical solution) explain the mechanism of fiber break at some distance in concrete volume, because during delamination growth elevated overstress is crossing different fiber cross-sections in concrete until the weakest is reached. Simultaneously overstress decreases with the distance from the crack (outer concrete block) surface and increase of fiber/matrix interface friction (corresponds to concrete matrix with higher compressive strength). These contrary factors describe the possibility to introduce “critical length” – parameter characterizing fiber anchoring capacity. At the same moment overloads in the matrix are growing into concrete body micro-cracks forming around the fiber. These cracks were observed experimentally. The third numerical model was elaborated to describe fiber sliding motion after the break in concrete matrix or delamination reach the embedded end of fiber. FEM model with contact elements between fiber and matrix was implemented. Fig. 3 (right picture) illustrates tensile stress (in fiber direction) in fiber and matrix during different stages of fiber pulling out of matrix with friction (friction coefficient value was 0.2). Stress distributions in the fiber, in this case, have the highest peak at the cross-section, the plane coinciding with outer surface of concrete block.

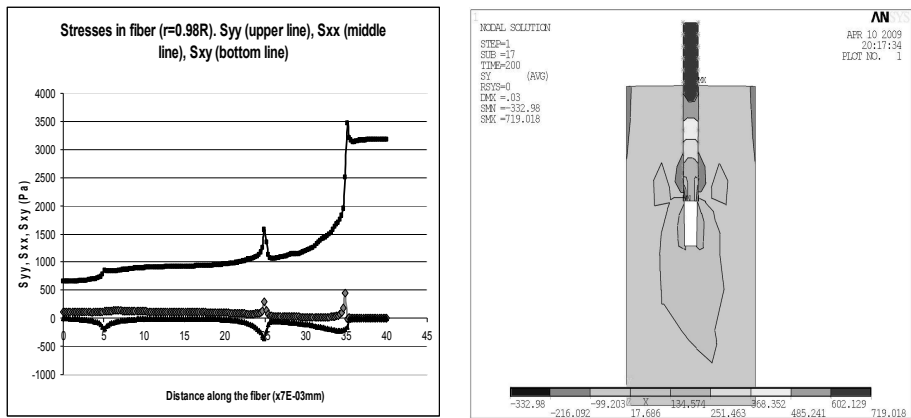


**Fig. 3.** Stresses in the fiber (kPa) on the line parallel to fiber direction (0.98R) (left picture). Stress in  $y$  direction along the fiber (upper line), stress in  $x$  direction – direction orthogonal to fiber direction (middle line) and shear stress (bottom line). Fiber sliding 2D FEM numerical modeling results. Between fiber and matrix are contact elements. Tensile stress in fiber direction in fiber and matrix (right picture) during different stages of fiber pulling out with friction

During pull-out process in the matrix longitudinal (in fiber direction) compressive stresses zones are generated, changing with tensile stresses when fiber end passes this place.

### Single glass fiber pulling out under an angle to embedment direction

Fibers cross cracks surfaces in concrete under different angles. This is why it is necessary to investigate pull-out micromechanics for inclined to tensile force fibers. 2D numerical

simulations were performed using ANSYS FEM software for single fiber pulled out of elastic volume under the angle  $\alpha \in [0^\circ, 70^\circ]$  to fiber embedment direction: with perfect bond between concrete and fiber; with partial debonding and sliding. Fig. 4 provides results for the fiber embedded under the angle  $\alpha = 30^\circ$  to stretching direction. Stress visualization indicates rupture possibilities for single elastic fiber bridging the crack: if bond between the fiber and matrix is perfect, one part of fiber breaks in cross-section coinciding with the concrete surface. At the same time stresses in concrete tend to cut the concrete matrix. Delamination started and for inclined fiber in concrete with partial debonding overloads are going Fig. 4 (left picture) inside the concrete block (similarly like for straight fiber). Fiber sliding tends to origination of micro-cracks in concrete around empty fiber channel in concrete Fig. 4 (right picture). Performed numerical simulations indicate the possibility to realize numerous failure micromechanical mechanisms for single elastic fiber pulling out of elastic matrix. At the same time it is important to conclude that elastic analysis is unable to describe micromechanics of metal (steel) fibers pulling out of concrete matrix, with deform elasto-plastically, as well as, more precise friction (between fiber and matrix) consideration leads to necessity of 3D molds.

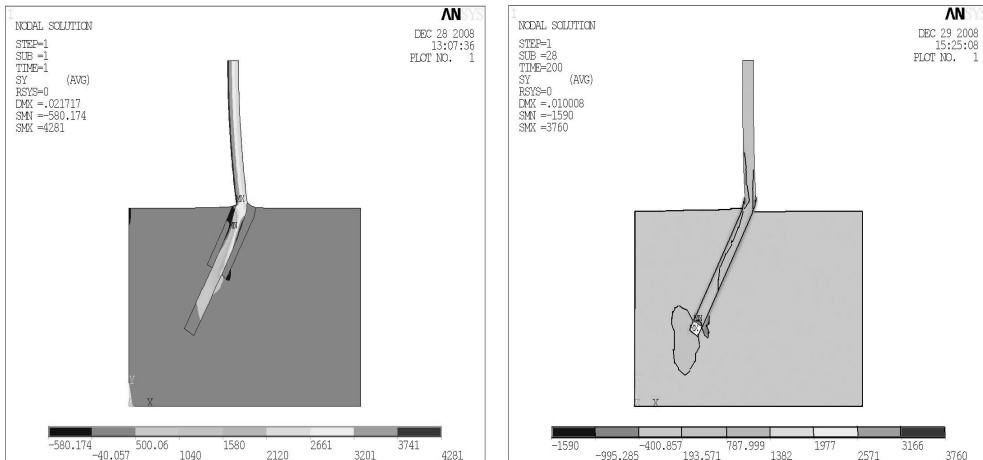


**Fig. 4.** Single elastic fiber pulling out under the angle  $\alpha = 30^\circ$  to fiber embedment direction. Fiber with partial delamination (left picture). Stress in vertical direction. Fiber is fully delaminated and is sliding with friction (right picture)

**Pull-out of single elasto-plastic fiber embedded orthogonally to elastic volume outer surface**

Single straight elasto-plastic fiber is oriented orthogonal to elastic volume (concrete) surface and is pulled out. 3D geometrical model was created using SolidWorks software (Fig. 5). Fiber is pulled out with friction out of matrix. Matrix shrinkage is taken into account. The problem is solved in the form of contact analysis. The complete pull-out process of fiber is modeled during which the displacement is applied to the loose fiber end. Fiber is debonded and the largest contribution to pull-out resistance is expected to occur from friction, which is magnified by the residual compression. Fiber slides with friction and is deformed elasto-plastically. According to symmetry only 1/4 of volume was observed. FEM model and the boundary conditions are represented in Fig. 5. One end of the model volume is rigidly clamped; outer cylindrical surface is under symmetry boundary conditions. Motion boundary conditions have been applied to the fiber loose end surface  $u = l_f$ . No penetration was specified between the fiber and the matrix and friction was also applied. Coulomb friction model was used (Fig. 6 (left picture)). The

results of numerical model were compared with experimental data for straight steel fibers pull-out with the length 50 mm and diameter 0.75 mm [16-18] with the goal to evaluate importance of the micromechanical processes such as fiber plasticity and fiber-matrix friction.

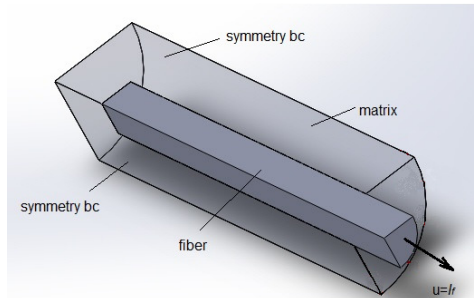


Fig. 5. FEM model (boundary conditions)

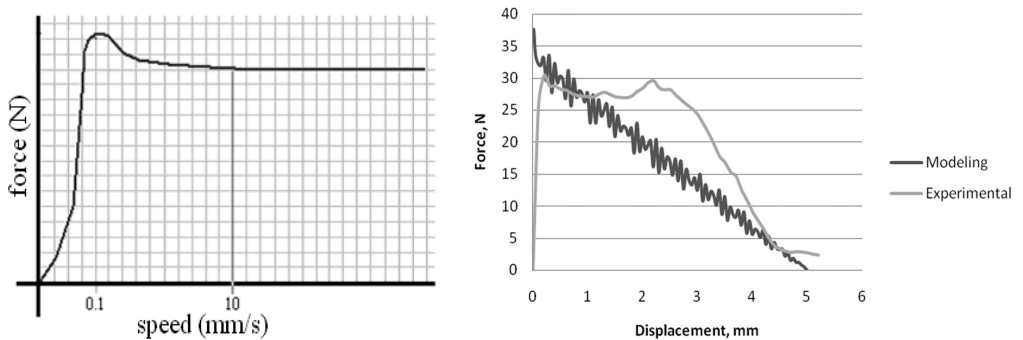


Fig. 6. Coulomb friction between fiber and matrix (left picture). Pull out modeling. Numerical modeling fitting the experimental curve for straight fiber embedded into matrix at the depth of 5 mm with concrete matrix shrinkage 0.09 % (right picture)

Applied force - pulling fiber displacement diagrams were numerically obtained and were compared with experimental data. Two parameters in the model were varied with the goal to more precisely approximate experimentally obtained curves: friction coefficient between steel fiber and concrete matrix as well as shrinkage of concrete. For macroscopic interaction friction coefficient between steel and concrete is known and is equal to 0.45. In the model we accepted the same value. The value of shrinkage was chosen by comparing the modeling results and experimental data for straight fiber embedded into matrix on the depth equal to 5 mm. Numerically into the matrix, with empty channel for the fiber, was introduced the fiber having the larger outer diameter than the inner diameter of the channel for the fiber. For example for concrete matrix shrinkage is equal to 0.09 %, the best fit was obtained when outer diameter of the fiber was 0.75 mm, but inner diameter of the channel in the matrix was equal to 0.7493 mm (Fig. 6 (right picture)).

### Single fiber is embedded at a different depth

The fiber was embedded into the matrix at a different depth: 5, 10, 15 and 20 mm. Data of performed pull-out experiments [15-18] is shown in Fig. 7 (left picture). Fibers were embedded at depth  $L$  into concrete straight and orthogonally to concrete volume outer surface and were

pulled out in direction coincident with the fiber. Numerical modeling simulations for fibers and matrix having the same mechanical properties are shown in Fig. 7 (right picture).

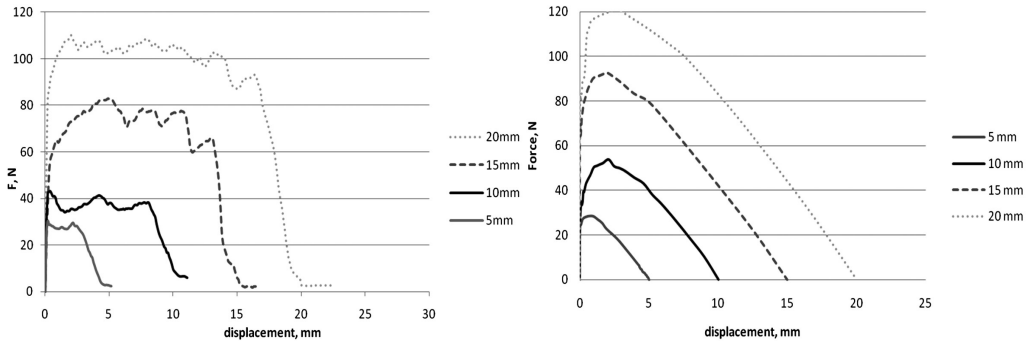


**Fig. 7.** Pull-out experimental data (left picture) for straight steel fibers embedded at different depth: 5 mm; 10 mm; 15 mm; 20 mm. Numerical modeling data for different embedded length (right picture)

Averaged curves over 9 tested samples are shown for every embedment depth value. Every experimental curve has typical parts. First (starting with pull-out displacement equal to zero and till 0.05-0.15 mm) part corresponds to elastic fiber deformation in elastic matrix with perfect bond between fiber and matrix. Curve is a straight line. This part is successfully modeled by the developed numerical model. The second part of the curve (starting from 0.05-0.15 mm to 0.5-0.6 mm on pull-out displacement axis) corresponds to delamination growth along fiber-matrix interface till full fiber debonding and partial motion with friction of its part (close to the loose fiber end) out of the matrix. Next part of the curve is concerned with fiber sliding with friction out of the matrix and partial plastic fiber deformation for fibers embedded into the matrix at high depth. At the beginning the curve is going up, applied force is increasing, after that at experimental curves we can recognize the “plato” – the curve part with practically constant applied pulling out force and growing pull-out displacement. Peaks and dimples on this curve part (like oscillations) can be explained by small concrete particles separation out of internal concrete surface by moving with friction fiber and plugs formation around the fiber out of these particles. Plug in the channel between fiber and matrix triggers fiber motion increased resistance to motion. After that the plug fails, thereby allowing fiber to move with decreasing applied pulling out load. Small particles in the channel between fiber and matrix roll after some time forming next plug (next peak on the curve). This plug formation process is dependent on fiber embedment depth (the higher the embedment depth, the more peaks we observe on the experimental curve), concrete matrix granulometry and matrix internal cohesion. Numerical model fails to approximate this part of the curve, because constant friction force was accepted at every two contact surfaces units along fiber and matrix. On the right picture applied pull-out forces are monotonically decreasing because during pull-out process every fiber surface that is in contact with the matrix decreases, when fiber is coming out of the matrix.

### Modeling for different inclination angle

Single straight elasto-plastic fiber is inclined (oriented under the angle) to tensile pulling out force. Force acting direction is oriented orthogonally to elastic volume (concrete) outer surface. 3D geometrical model was built using SolidWorks software (Fig. 8). Fiber is pulling out of matrix with friction.

Matrix shrinkage is not taken into account. The problem is solved in the form of contact analysis. The complete pull-out process of fiber is modeled till the moment when the complete fiber embedded end is pulled out of the matrix. According to symmetry only half of the fiber in

matrix was observed. Growing displacement is applied to the loose fiber end. Fiber is debonded. Coming out of the elastic matrix, the fiber deforms elasto-plastically. Such contribution in pull-out resistance is formed by friction between fiber and matrix as well as elasto-plastic fiber bending. Friction is magnified by the residual compression due to matrix shrinkage. Numerical calculations were performed for steel fiber in concrete matrix (performing fitting procedure according to shrinkage of concrete matrix). Elasto-plastic fiber material deformation diagram is provided in Fig. 9. Present stress in the fiber exceeds the yield stress of steel. Therefore, large displacement study was used for pull out curve modeling. Plasticity von Misses model was used for simulations. Stress-strain curves were obtained experimentally for fibers embedded at different depth and were oriented under different angle to applied pulling out force.

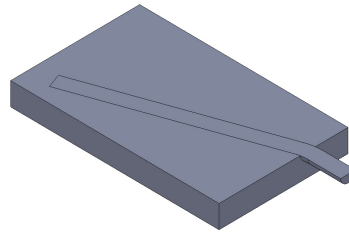


**Fig. 8.** Pull out model for different inclination angle

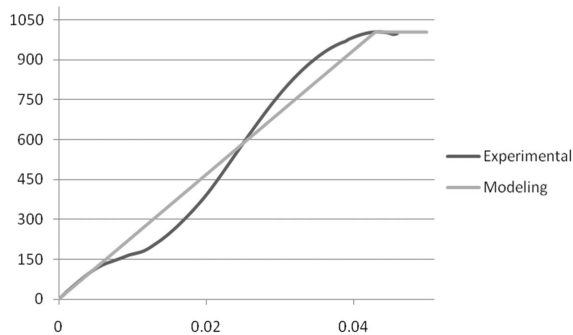


**Fig. 9.** Fiber elasto-plastic stress strain diagram

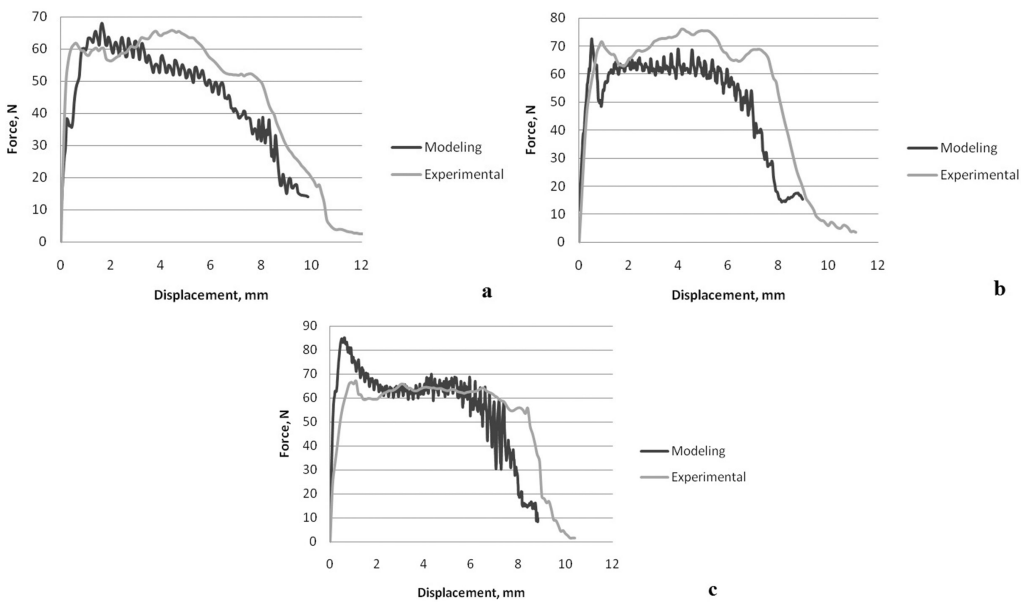
Experimental and modeling curves for straight rounded steel fibers with the length of 50 mm and diameter 0.75 mm were embedded into the matrix on a depth: 10 mm and oriented under angles: a) – 20°, b) – 45° and c) – 60° degrees to applied pulling force are shown in Fig. 10a, b, c.

Fig. 11a, b provide experimental and numerical results for the fiber oriented under the angle 20° to applied force direction and embedded at different depth into matrix: a) – 15 mm; b) – 25 mm. Comparison of experimental data and numerical results indicates that implementation of two nonlinear processes: fiber-matrix friction and plastic deformation of fiber into single fiber pull-out micromechanics allows correctly predict this process by changing its parameters (angle and embedment depth) in a wide range. At the same time, for model improvement, plugging process of concrete particles must be included into the consideration as well.

## Conclusions

Detailed 2D numerical investigation of elastic (glass, carbon) single fiber pull-out of concrete matrix was performed. Simulation results were compared with the experimental

findings. Major fiber load bearing and rupture mechanisms were considered. Detailed 3D finite element analysis was conducted for elasto-plastic single fiber pull-out of concrete matrix. Simulations results were compared with the performed experiments. It was demonstrated that model based on assumptions on friction between fiber and matrix and elastic fiber and matrix deformations fail to reproduce the experimental curves. Micro-mechanical mechanism of small concrete particles separation out of internal fiber channel surface in concrete due to fiber friction and plugs formation around the fiber must be taken into account. Plug in the channel between fiber and matrix triggers fiber motion increased resistance to motion. After that the plug fails, allowing fiber to move simultaneously decreasing applied pulling load. Small particles in the channel between fiber and matrix are rolled after some time forming next plug. Numerical simulations indicate that in situation, when fiber is inclined to acting force direction, this plugging process importance decreases in comparison with other nonlinear processes such as friction and plastic deformations.



**Fig. 10.** Experimental and modeling curves for fibers embedded into the matrix at a depth of 10 mm.  
 a) Fiber is oriented under the angle of  $20^\circ$  to applied force direction;  
 b) Fiber is oriented under the angle of  $45^\circ$  to applied force direction;  
 c) Fiber is oriented under the angle of  $60^\circ$  to applied force direction

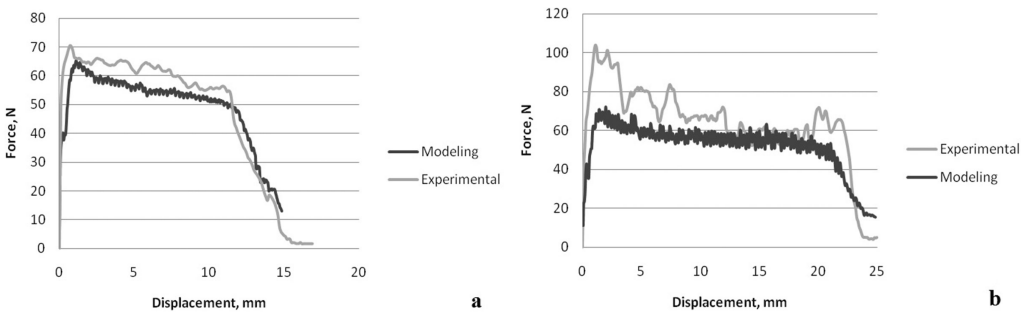


**Fig. 11.** Experimental and numerical curves for fibers oriented under the angle of  $20^\circ$  to applied force direction.  
 a) Fiber is embedded into the matrix at a depth of 15 mm;  
 b) Fiber is embedded into the matrix at a depth of 25 mm

## References

- [1] **Li C., Mobasher B.** Finite element simulations of fiber pull-out toughening in fiber reinforced cement based composites. *Journal of Advanced Cem. Based Mater.*, Vol. 7, No. 3 – 4, 1998, p. 123 – 132.
- [2] **Mobasher B., Li C.** Modelling of stiffness degradation of the interfacial zone during fiber debonding. *Journal of Compos. Eng.*, Vol. 5, No. 10 – 11, 1995, p. 1349 – 1365.
- [3] **Tsai J., Patra A., Wetherhold R.** Finite element simulation of shaped ductile fiber pull-out using a mixed cohesive zone/friction interface model. *Compos. Part A, Appl. Sc. Manuf.*, Vol. 36, No. 6, 2005, p. 827 – 838.
- [4] **Krasnikovs A., Khabaz A., Kononova O.** Numerical 2D investigation of non-metallic (glass and carbon) fiber micro-mechanical behaviour in concrete matrix. *Sc. Proceedings of Riga Technical University, Architecture and Construction Science 2*, Vol. 10, 2009, p. 67 – 78.
- [5] **Krasnikovs A., Kononova O.** Strength prediction for concrete reinforced by different length and shape short steel fibers. *Sc. Proceedings of Riga Technical University, Transport and Engineering 6*, Vol. 31, 2009, p. 89 – 93.
- [6] **Krasnikovs A., Khabaz A., Telnova I., Machanovsky A., Klavinsh I.** Numerical 3D investigation of non-metallic (glass, carbon) fiber pull-out micromechanics (in concrete matrix). *Sc. Proceedings of Riga Technical University, Transport and Engineering 6*, Vol. 33, 2010, p. 103 – 108.
- [7] **Stang H.** In *Fracture of Brittle, Disordered Materials: Concrete, Rock and Ceramics*. Baker G., Karihaloo B. L. Eds., E&FN Spon: London, 1995, p. 131 – 148.
- [8] **Li V.** *ASCE J., Mater. Civil Eng.*, Vol. 4, 1992, p. 41 – 57.
- [9] **Li V., Stang H., Krenchel H.** *Mater. Struct.*, Vol. 26, 1993, p. 486 – 494.
- [10] **Stang H., Li V., Krenchel H. J.** *Mater. Struct.*, Vol. 28, 1995, p. 210 – 219.
- [11] **Hutchinson J. W., Jensen H. M.** Models of fiber debonding and pullout in brittle composites with friction. *Journal of Mechanics of Materials*, Vol. 9, 1990, p. 139 – 163.
- [12] **Jones P. A., Austin S. A., Robins P. J.** Predicting the flexural load–deflection response of steel fiber reinforced concrete from strain, crack-width, fiber pull-out and distribution data. *Journal of Materials and Structures*, 2008, p. 449 – 463.
- [13] **Robins P., Austin S., Jones P.** Pull-out behaviour of hooked steel fibers. *Materials and Structures*, Vol. 35, 2002, p. 434 – 442.
- [14] **Bentur A., Wu S., Banthia N., Baggott R., Hansen W., Katz A., Leung C., Li V., Mobasher B., Naaman A., Robertson R., Soroushian P., Stang H., Taerwe L.** In *High Performance Fiber Reinforced Cementitious Composites*. Naaman A., Reinhardt H. Eds., London, 1995, p. 149 – 191.
- [15] **Li V., Maalej M.** *Cem. Concr. Compos.*, Vol. 18, 1996, p. 239 – 249.
- [16] **Georgiadi-Stefanidi K., Mistakidis E., Pantousa D., Zygomalas M.** Numerical modeling of the pull-out of hooked steel fibers from high-strength cementitious matrix, supplemented by experimental results. *Constr. Build. Mater.*, Vol. 24, 2010, p. 2489 – 2506.
- [17] **Pupurs A., Krasnikovs A., Kononova O., Shakhmenko G.** Non-linear post-cracking behavior prediction method for high concentration steel fiber reinforced concrete (HCSFRC) beams. *Scientific Proceedings of Riga Technical University, Construction Science*, 2007, p. 60 – 70.
- [18] **Krasnikovs A., Pupurs A.** High-performance steel fiber reinforced concrete (SFRC) fracture. Fiber pull-out experimental investigation. *Scientific Proceedings of 8th International Symposium on Utilization of High-Strength and High-Performance Concrete*, October 27 – 29, 2008, Tokyo, Japan, 2008, p. 161 – 170.
- [19] **Pupurs A.** Prediction of Load Bearing Capacity of Structural Steel Fiber Reinforced Concrete. *Doctoral Theses, Riga Technical University*, 2011, p. 149.
- [20] **Rozite L.** High Strength Fiberconcrete Use in Structural Elements Subjected to Bending. *M. Sc. Theses, Riga Technical University*, 2009, p. 51.
- [21] **Pupurs A., Varna J.** Fracture mechanics analysis of debond growth in a single-fiber composite under cyclic loading. *Mechanics of Composite Materials*, Vol. 47, No. 1, 2011, p. 109 – 124.